Environmental Toxicology and Pharmacology 66 (2019) 116–125

Contents lists available at ScienceDirect

Environmental Toxicology and Pharmacology

journal homepage: www.elsevier.com/locate/etap

Pulmonary effects of nanofibrillated celluloses in mice suggest that carboxylation lowers the inflammatory and acute phase responses

Niels Hadrup[a,1], Kristina Bram Knudsen[a,1], Trine Berthing[a], Henrik Wolff[b], Stefan Bengtson[a], Christian Kofoed[c], Roall Espersen[c], Casper Højgaard[c], Jakob Rahr Winther[c], Martin Willemoës[c], Irene Wedin[d], Markus Nuopponen[e], Harri Alenius[f,g], Hannu Norppa[b], Håkan Wallin[h], Ulla Vogel[a,i,*]

[a] National Research Centre for the Working Environment (NFA), 105 Lersø Parkallé, Copenhagen Ø, Denmark
[b] Finnish Institute of Occupational Health (FIOH), P.O. Box 40, 00032, Työterveyslaitos, Helsinki, Finland
[c] Section for Biomolecular Sciences, Department of Biology, University of Copenhagen, Denmark
[d] Stora Enso, Finland
[e] UPM Kymmene Oyj, Finland
[f] Department of Bacteriology and Immunology, University of Helsinki, Finland
[g] Institute of Environmental Medicine (IMM), Karolinska Institutet, Sweden
[h] National Institute of Occupational Health, Oslo, Norway
[i] Department of Micro- and Nanotechnology, Danish Technical University (DTU), DK-2800, Kgs., Lyngby, Denmark

ARTICLE INFO

Keywords:
Nanoparticle
Nanomaterial
Genotoxicity
Neutrophils
Serum amyloid A
Nanocellulose

ABSTRACT

We studied if the pulmonary and systemic toxicity of nanofibrillated celluloses can be reduced by carboxylation. Nanofibrillated celluloses administered at 6 or 18 μg to mice by intratracheal instillation were: 1) FINE NFC, 2–20 μm in length, 2–15 nm in width, 2) AS (−COOH), carboxylated, 0.5–10 μm in length, 4–10 nm in width, containing the biocide BIM MC4901 and 3) BIOCID FINE NFC: as (1) but containing BIM MC4901. FINE NFC administration increased neutrophil influx in BAL and induced SAA3 in plasma. AS (−COOH) produced lower neutrophil influx and systemic SAA3 levels than FINE NFC. Results obtained with BIOCID FINE NFC suggested that BIM MC4901 biocide did not explain the lowered response. Increased DNA damage levels were observed across materials, doses and time points. In conclusion, carboxylation of nanofibrillated cellulose was associated with reduced pulmonary and systemic toxicity, suggesting involvement of OH groups in the inflammatory and acute phase responses.

1. Introduction

Nanofibrillated cellulose can be described as a dense network of highly fibrillated cellulose ranging from 10 to 100 nm in width and up to several micrometres in length (Johnson et al., 2009; Vartiainen et al., 2011). Nanofibrillated cellulose has been reported as an ingredient in paper, building materials, food, cosmetics, and pharmaceutical products (Gómez et al., 2016). During the manufacturing of nanofibrillated cellulose, workers are potentially exposed during procedures such as grinding, spraying or drying (Vartiainen et al., 2011).

Nanofibrillated cellulose is a subset of cellulose, and therefore literature on the toxicity of cellulose and cellulose-containing dusts constitutes a starting point for the understanding of its toxicity. Exposure to wood dust causes cancer of the nose and the paranasal sinuses (IARC, 1995), and exposure to textile fibres in weavers is possibly carcinogenic (Muhle and Ernst, 1997; IARC, 1990). Occupational exposure to cotton dust that primarily consists of cellulose has been linked to the development of chest tightness, bronchial hyperresponsiveness and chronic

Abbreviations: BAL, bronchoalveolar lavage fluid; Bw, body weight; LPS, lipopolysaccharide; SAA, serum amyloid A

* Corresponding author at: National Research Centre for the Working Environment, Lersø Parkallé 105, DK-2100, Copenhagen Ø, Denmark.
E-mail addresses: nih@nfa.dk (N. Hadrup), bramknudsen@gmail.com (K.B. Knudsen), trb@nfa.dk (T. Berthing), henrik.wolff@ttl.fi (H. Wolff), stefan.bengtson@thermofisher.com (S. Bengtson), christian.kofoed@chem.ku.dk (C. Kofoed), roes@bio.dtu.dk (R. Espersen), casperhoejgaardmail@gmail.com (C. Højgaard), jrwinther@bio.ku.dk (J.R. Winther), willemoes@bio.ku.dk (M. Willemoës), Irene.Wedin@storaenso.com (I. Wedin), markus.nuopponen@upm.com (M. Nuopponen), Harri.Alenius@helsinki.fi, Harri.Alenius@ki.se (H. Alenius), hannu.norppa@ttl.fi (H. Norppa), Hakan.Wallin@stami.no (H. Wallin), ubv@nfa.dk (U. Vogel).
[1] N.H. and K.B.K. contributed equally to this publication.

https://doi.org/10.1016/j.etap.2019.01.003
Received 9 January 2019; Accepted 13 January 2019
Available online 14 January 2019

bronchitis (Rylander et al., 1987). Exposure of rats to cellulose dust by inhalation at 1000 fibres/mL (corresponding to 116 mg/m^3, assuming that 10^8 fibres weigh 11.6 mg) 7 h/day for 1 to 14 days induced a pulmonary inflammatory response that peaked on day 1 (Cullen et al., 2000). Hamsters were exposed to cellulose dust by intratracheal instillation of 7.5 mg/kg bw. Eight weeks later, granulomas and thickened inter-alveolar septae were observed in the lungs (Milton et al., 1990). Cellulose is cleared from the lung slowly as cellulose fibres administered to rats by intratracheal instillation (˜6 mg/kg bw) were found to have an elimination half-life of ˜1000 days (Muhle and Ernst, 1997).

Concerning studies specifically on nanosized cellulose,[2] mice were exposed to 2,2,6,6-tetramethyl-piperidin-1-oxyl oxidised nanofibrillated cellulose (300–1000 nm in length, 10–25 nm in width) by pulmonary aspiration. The doses were 10, 40, 80 and 200 μg/mouse. This resulted in increased numbers of inflammatory cells, e.g. neutrophils, in bronchoalveolar lavage fluid (BAL), and increased levels of DNA damage in the lung; mRNA levels of inflammatory cytokines and chemokines were also elevated. The accumulation of nanofibrillated cellulose was dose related and was detected in the bronchi, the alveoli and, to a lesser extent, macrophages (Catalán et al., 2017). In another study, mice were exposed to cellulose nanocrystals (158 nm in length, 54 nm in width) by pharyngeal aspiration. The dose was 10 μg/mouse 2 times a week for 3 weeks. This resulted in impaired pulmonary function, pulmonary inflammation and damage, oxidative stress, increased TGF-β and elevated collagen levels in lung tissue (Shvedova et al., 2016). Yanamala et al. exposed mice to two different forms of cellulose nanocrystals derived from wood (CNCS: 90 nm in length and 7 nm in width; CNCP: 208 nm in length and 8 nm in width). The exposure was via pharyngeal aspiration, and the doses were 50, 100, and 200 μg/mouse. This resulted in increased numbers of leukocytes and eosinophils in BAL. Tissue damage biomarkers were affected to different extent among the two forms as were the levels of oxidatively modified proteins and inflammatory cytokines (Yanamala et al., 2014). In a study of (Farcas et al., 2016), mice were exposed to cellulose nanocrystals (158 nm in length, 54 nm in width) by pharyngeal aspiration (40 μg/mouse 2 times a week for 3 weeks). A range of testes effects were observed: perturbed sperm concentration, motility, morphology, and DNA integrity, increased pro-inflammatory cytokine levels in the testes, and induction of oxidative stress in the testes and epididymis, damage to testicular structure, and perturbed levels of testosterone and luteinizing hormone (Farcas et al., 2016). Ilves et al. investigated the effects of 5 celluloses in mice by oropharyngeal aspiration. Two of the materials, FINE NFC and AS (−COOH; with BIM MC4901 biocide), are also investigated in the current study. The other celluloses were bulk sized cellulose, a carboxymethylated NFC (2–50 μm in length, 3–10 nm in width) containing fibril bundles, and an NFC of 0.5 to 10 μm in length and 4–10 nm in width containing fibril bundles. The doses were 10 or 40 μg/mouse (˜0.5 and ˜2 mg/kg bw). All 5 materials increased neutrophil numbers in BAL at both doses. However the non-functionalised materials were evaluated to be more prone to trigger inflammation than those functionalised by carboxymethylation (Ilves et al., 2018).

We have previously shown that pulmonary exposure to nanomaterials including particles and fibres induce a pulmonary acute phase response in parallel with the pulmonary inflammatory response (Poulsen et al., 2015a, b; Saber et al., 2013). Increased blood levels of acute phase response proteins Serum Amyloid A (SAA) and C-reactive protein (CRP) are risk factors for cardiovascular disease in prospective epidemiological studies (Gabay and Kushner, 1999; Ridker et al., 2000). In mice, Serum Amyloid A3 (*Saa3*) was found to be the most differentially regulated acute phase gene following pulmonary exposure to nanomaterials (Bourdon et al., 2012; Halappanavar et al., 2011; Poulsen et al., 2015a; Saber et al., 2014). In addition, pulmonary *Saa3* mRNA levels correlated closely with neutrophil influx and with blood levels of SAA3 (Poulsen et al., 2017). SAA is causally related to atherosclerosis. Inactivation of all three inducible SAA isogenes leads to lowered plaque progression in APOE mice, whereas overexpression of SAA1 or SAA3 increases plaque progression (Dong et al., 2011; Thompson et al., 2018).

In prioritising different forms of nanofibrillated cellulose for future use, differences in toxicity should be exploited for safe-by-design considerations. Nanofibrillated cellulose appears to be highly inflammogenic 24 h following pulmonary exposure (Ilves et al., 2018). We therefore expected that nanofibrillated cellulose would also induce a strong acute phase response. We have previously noted that graphene oxide was much more inflammogenic and induces more acute phase response than reduced graphene oxide (Bengtson et al., 2017). In addition, lipopolysaccharide (LPS) induces strong inflammatory and acute phase responses and we expect that the overall structural resemblance between cellulose and LPS may explain the strong induction of inflammation and acute phase responses; we therefore hypothesised that blocking of the OH groups would reduce cellulose-induced inflammation and acute phase responses. In the current study, the pulmonary toxicity was studied in mice with intratracheal instillation of three different forms of nanofibrillated cellulose. The tested nanofibrillated celluloses were 1) FINE NFC 2–20, μm in length, 2–15 nm in width, 2) AS (−COOH), 0.5–10 μm in length and 4–10 nm in width, with carboxylated OH groups and impregnated with the biocide BIM MC4901; And in order to determine whether this biocide had an effect: 3) BIOCID FINE NFC (FINE NFC impregnated with BIM MC4901). The endpoints investigated were pulmonary inflammation, systemic acute phase response, genotoxicity, and histopathology of the lungs and livers. Our results on inflammation and the systemic acute phase response support the hypothesis that the carboxylation of OH groups reduces the toxicity of nanofibrillated cellulose.

2. Materials and methods

2.1. Nanofibrillated celluloses

Three nanofibrillated cellulose materials were used: 1) FINE NFC, 2–20 μm in length, 2–15 nm in width, 2) BIOCID FINE NFC, i.e. FINE NFC impregnated with the biocide BIM MC4901, and 3) AS (−COOH), 0.5–10 μm in length and 4–10 nm in width, also impregnated with BIM MC4901. These materials were produced from natural wood-based pulp by Stora Enso Oyj and UPM Kymmene Oyj (Finland) and were provided by the manufacturers. Material characteristics are presented in Table 1 and have previously been described in detail (Knudsen et al., 2015). Both BIOCID FINE NFC and AS (−COOH) preparations contained the biocide BIM MC4901, a mixture of 5-chloro-2-methyl-2H-isothiazol-3-one and 2-methyl-2H-isothiazol-3-one (ECHA, 2013). In the BIM MC 4901 safety data sheet from the manufacturer of the nanofibrillated cellulose, it is stated that the composition of BIM MIC4901 is 80–90% of water, 1–2.9% of magnesium nitrate (CAS number 10377-60-3), 1–2.5% of 5-chloro-2-methyl-2H- isothiazol-3-one and 2-methyl-2H-isothiazol-3-one (CAS number: 55965-84-9), and < 0.2% Copper(II) nitrate (CAS number: 3251-23-8).

2.2. Dispersion of nanofibrillated celluloses in instillation vehicle

The nanomaterials were dispersed in filtered water (resistivity of 18.2 MΩ cm) containing 2% serum from sister mice by shaking followed by vigorous vortexing for 10 min resulting in a 4 mg/ml stock dispersion. Subsequently the dispersions were sonicated on ice-bath for 16 min using a Branson Sonifier S-450D (Branson Ultrasonics Corp., Danbury, CT) equipped with a 13 mm disruptor horn (Model number: 101-147-037, Branson Ultrasonics Corp., Danbury, CT, USA). The dispersions were used immediately, and a short vortexing step was applied to the dispersions immediately before the administration.

[2] We retained the material designations used in the individual articles.

Table 1
Overview of nanofibrillated cellulose materials used in this study.

Material	Concentration in stock solution (% in water)	Length (μm)	Width (nm)	Aspect ratio	Zeta potential (mV)	Remarks
FINE NFC	2.35	2–20	2–15	100–1000	−15	Enzymatic pre-treatment with cellulase; Hemicellulose content 17% (weight)
BIOCID FINE NFC	2.50	2–20	2–15	100–1000	−15	FINE-NFC impregnated with 12.5 mg/kg of the biocide BIM MC 4901 (CAS number 55965-84-9)
AS (-COOH) also designated: Nanocellulose –UPM Biofibrils AS	2.47	0.5–10	4–10	100–1000	−25	Carboxylated 70% crystallinity structure 19% (weight) hemicellulose Impregnated with 12.5 mg/kg of the biocide BIM MC 4901 (CAS number 55965-84-9)

2.3. Animal housing and permission

Female C57BL/6 mice were obtained from Scanbur AB (Karlslunde, Denmark). The mice were 7–8 weeks old at arrival and were housed in groups of 6–7 mice per cage in humidity and temperature-controlled ventilated rooms with a 12 h day/night cycle (the light was on from 6 A M to 6 PM). A standard rodent diet (Altromin no. 1314 FORTI, Altromin Spezialfutter GmbH & Co., Germany) and water were provided *ad libitum*. Housing was in Makrolon type III propylene cages with Enviro-dry bedding (Brogaarden, Gentofte, Denmark). Enrichment was plastic hides and wood blocks. The animals were allowed to acclimatize for 5 days. Cage-side clinical observations were conducted on a daily basis during the acclimatization period as well and during the study. All animal procedures complied with the EC Directive 86/609/EEC and Danish law regulating experiments with animals (The Danish Ministry of Justice, Animal Experiments Inspectorate permissions 2010/561-1779 and 2015-15-0201-00465. Intratracheal instillation was done as previously described (Jacobsen et al., 2009).

2.4. Study 1: dose finding study of FINE NFC and AS (−COOH)

The mice were dosed by intratracheal instillation with 128 μg /mouse of FINE NFC and AS (−COOH). Two mice were used per material.

2.5. Study 2: comparison study of FINE NFC and AS (−COOH)

The aim of this study was to compare FINE NFC and AS (−COOH). The dose levels were 6 and 18 μg/mouse. N was 7 per group for bronchoalveolar lavage fluid (BAL) analysis, and an additional 6 mice were utilized for histology. The materials were administered by single intratracheal instillation using a 50 μl volume (0.12 or 0.36 mg material/mL). The animals were humanely killed 24 h or 28 days post exposure. Two animals served as controls for histology for each time point. Concerning controls, the animal experiment in which these two nanofibrillated celluloses were investigated also included 16 other nanomaterials, the data of which are not reported here. The different materials were instilled on separate (but sequential) days, and on each day 2–3 controls were included for both time points (1 and 28 days). In the evaluation of the results in the current report, we included all controls in the whole study. For BAL cellularity and for the assessment of DNA strand breaks, this enabled a control group of 48 mice on day 1 and 30 mice on day 28; for *Saa3* mRNA level data this enabled 26 controls on day 1 and 16 controls on day 28.

2.6. Study 3: evaluation of the effect of biocide treatment of the nanofibrillated cellulose

For evaluation of the biocide treatment, FINE NFC administration was compared with BIOCID FINE NFC administration for cellularity of BAL and for analysis of DNA strand breaks. Only one dose level, 18 μg/mouse, was applied by intratracheal instillation (50 μl of 0.36 mg material/mL). N was 6 per group. The animals were humanely killed 24 h post exposure. A control group of 6 mice was included in the investigation.

2.7. Necropsy

The mice were weighed and anesthetized by an IP injection with a ZRF cocktail (Zoletil Forte 250 mg, Rompun 20 mg/ml, Fentanyl 50 μg/ml in sterile isotone saline, dose 0.1 ml/25 g bodyweight). Animals dedicated for BAL and genotoxicity assessment had heart blood withdrawn (stabilized with K_2EDTA) after which the lungs were flushed twice with 0.8 ml sterile 0.9% NaCl to obtain bronchoalveolar lavage (BAL). Heart, lung and liver tissue were recovered, cut into appropriate pieces, added to cryotubes and snap frozen in liquid nitrogen. The

samples were stored at −80 °C until further analyses. From the animals dedicated for histology, pieces of the lung and liver were recovered and fixed in formalin.

2.8. Cellular composition of BAL

BAL fluid recovered from the animals was stored on ice until division into a cellular and a fluid fraction by centrifugation at 400 *g* for 10 min at 4 °C. The acellular BAL fluid was stored in aliquots at −80 °C until analysis. The BAL cells were re-suspended in 100 µl HAM F-12 cell culture medium (HAM F-12 with 1% penicillin/streptomycin and 10% foetal bovine serum). The total number of living and dead cells in BAL was determined with a NucleoCounter NC-200TM (Chemometec, Denmark) according to the manufacturer's protocol. Samples for the comet assay were prepared by combining 40 µl re-suspended BAL cells with 60 µl HAM F12 freezing medium (HAM F12, 1% penicillin/streptomycin, 15% foetal bovine serum, and 10% DMSO). Aliquots were transferred to −80 °C until analysis. The remaining cell resuspension volume (40 µl) was used to estimate the numbers of granulocytes (neutrophils and eosinophils), macrophages, lymphocytes and epithelial cells in the BAL fluid. For this, the cell suspension was centrifuged at 55 *g* for 4 min in a Cytofuge 2 (StatSpin, TRIOLAB, Brøndby, Denmark) and fixed for 5 min in 96% ethanol. The slides were then stained with May-Grünwald-Giemsa stain, randomized and blinded before the counting of 200 cells per sample under a microscope using a 100x magnification.

2.9. Histology and immunohistochemistry procedures

The rat lungs recovered from Study 2 were slowly filled with 4% formalin under a 30 cm water column pressure. A knot was tied on trachea to secure sufficient formaldehyde to fixate tissue in 'inflated state' of the lung. The lungs as well as the livers were fixed in 4% formalin for at least 24 h and next the formalin fixed samples were trimmed, dehydrated and embedded in paraffin. Sections were cut at a thickness of 3 µm. For the evaluation of general morphology, the sections were stained with the haematoxylin and eosin (H&E) stain. Next the sections were evaluated for histopathological changes under light microscope. The groups evaluated were vehicle (control), 18 µg/mouse FINE NFC, and 18 µg/mouse AS (−COOH) on 28 days after the exposure. For the evaluation of cellulose in the lungs and liver of 3 mice of each cellulose groups and 2 vehicle control mice, the EXG:CBM staining was done as detailed previously (Knudsen et al., 2015). In brief, paraffin was removed from the sections by a PBS wash. Endogenous peroxidase was blocked with Ultravison Hydrogen Peroxide Block, (Thermo scientific, Fremont CA, USA) for 10 min. After washing with PBS, 30% rabbit normal serum with avidin from the Avidin /Biotin Blocking Kit (Vector Laboratories, Burlingame, CA, USA) was applied to the sections for 30 min and then gently removed by washing in PBS. Biotinylated EXG 1 mg/ml was applied to the sections at a dilution of 1:300 and incubated for 60 min. After washing with PBS, streptavidin-peroxidase (Rockland, Limerick, PA, USA) was applied to the sections at a dilution of 1:300 of 1 mg/mL. After incubation for 30 min and another PBS wash, Large Volume AEC Chromogen Single Solution (Thermo Scientific) was applied for 5 min. The sections were counterstained with Mayer's haematoxylin, dried and mounted for microscopy. Images were acquired at 20x magnification using an Olympus BX 43 microscope with a 0.5x C-mount and a Nikon DS-Fi2 camera. Image contrast was adjusted in Adobe Photoshop to visualise the faint haematoxylin-stained nuclei together with the intense EXG:CBM-stained cellulose.

2.10. Analysis of DNA strand break levels by comet assay

DNA strand break levels were analysed in the comet assay and presented as percentage of DNA in the comet tail of single cells. The comet assay was done as described previously (Jackson et al., 2013). In brief, BAL cells preserved in freezing media were thawed in a 37 °C water bath. Lung and liver tissue samples were homogenized in Merchant's medium (140 mM NaCl 1.5 mM KH_2PO_4, 2.7 mM KCl, 8.1 mM Na_2HPO_4, 10 mM Na_2EDTA, pH 7.4). The cells were then suspended in agarose heated to 37 °C (at a final agarose concentration of 0.7%), and embedded on Trevigen CometSlides™. Cooled slides were placed overnight in a lysis buffer at 4 °C. The slides were rinsed in electrophoresis buffer and alkaline treated for 40 min. Electrophoresis was run for 25 min under buffer circulation (70 mL/min) at an applied voltage of 1.15 V/cm and a current of 300 mA. The slides were neutralised (2 x 5 min), fixed in 96% ethanol for 5 min and then placed on a 45 °C heating plate for 15 min. The cells were stained in 20 mL/slide bath with TE buffered SYBR®Green fluorescent stain for 15 min and dried at 37 °C for 10 min. UV-filter and cover slip were applied, and DNA damage was analysed using the IMSTAR Pathfinder™ system. The results are presented as an average percentage tail DNA value for all cells scored in each Trevigen CometSlide well. The day-to-day variation and electrophoresis efficiency was validated by including wells of A549 epithelial lung cells exposed to PBS or 60 µM H_2O_2 on each slide. These served as negative and positive historical controls, respectively.

2.11. Measurement of SAA3 protein levels in blood plasma

ELISA analysis specifically targeting plasma SAA3 levels was conducted in accordance with the manufacturer's instructions (Mouse Serum Amyloid A-3, Cat.#EZMSAA3-12 K, Millipore) and has been described in detail by (Poulsen et al., 2017, 2015a).

2.12. Statistical analysis

Data were analysed using Graph Pad Prism 7.02 software package (Graph Pad Software Inc., La Jolla, CA, USA). Data were tested by one-way ANOVA with Sidak's multiple comparisons test (one-way ANOVA). Groups that were simultaneously compared by Sidak's multiple comparisons test were: for Animal Study 2: All treatment groups vs. vehicle (control); FINE NFC 6 µg vs. AS (−COOH) 6 µg; FINE NFC 18 µg vs. AS (−COOH) 18 µg; and for Animal Study 3: all three groups against each other.

3. Results

3.1. Dose finding study

Exposure of mice to 128 µg/mouse (6.4 mg/kg bw) of FINE NFC or AS (−COOH) resulted in difficulty of breathing and distress within 3 h after intratracheal instillation; and therefore the animals were immediately humanely killed. Based on these results the highest dose for the subsequent animal experiments was set to 18 µg/mouse (0.9 mg/kg bw).

3.2. Pulmonary inflammation determined by increased neutrophil numbers in BAL

On day 1, exposure to FINE NFC and AS (−COOH) resulted in dose-dependent increases of the number of neutrophils in BAL. The responses were higher to FINE NFC than to AS (−COOH) (Fig. 1A). On day 28, both doses of FINE NFC as well as the lowest dose of AS (−COOH) resulted in increased numbers of neutrophils in BAL (Fig. 1B). To exclude the possibility that the lower inflammatory response induced by AS (−COOH) was caused by the BIM-MC4901 biocide, the inflammatory potential of FINE NFC with and without this biocide was compared at day 1 at 18 µg/mouse. At this dose, there was an increase of neutrophils for both materials as compared to control. The response to BIOCID FINE NFC was higher than that observed after the FINE NFC exposure (Fig. 1C), and thus the reduced inflammatory response induced by AS (−COOH) was not explained by the presence of the

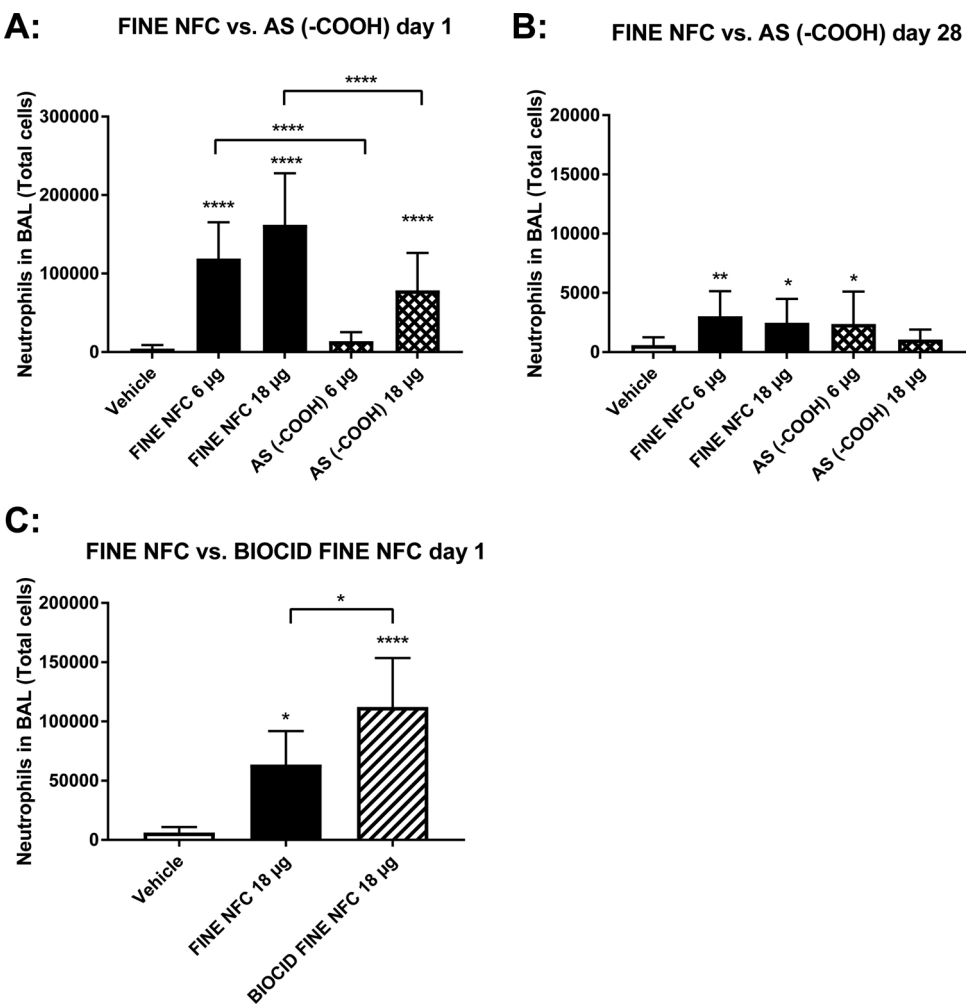

Fig. 1. Total neutrophil influx into BAL fluid. Nanofibrillated cellulose materials were administered to mice by intratracheal instillation. Panel A and B: day 1 and -28 post exposure to FINE NFC and AS (−COOH), 6 or 18 µg/mouse. The values represent mean of all animals in the group ± SD (n = 7); Panel C: day 1 post exposure to FINE NFC and BIOCIDE FINE NFC. The values represent mean of all animals in the group ± SD (n = 6). ****,**, ** and * designates *p* values of < 0.0001, < 0.01 and < 0.05 respectively *vs.* vehicle or in case of the insertion of a lateral bar: treatment *vs.* treatment by Sidak's multiple comparisons test (one-way ANOVA).

biocide. A number of other cell types in BAL as well as the total cell number in BAL were affected by the exposure to NFC and AS (−COOH) (Table 2).

3.3. SAA3 level in blood plasma

Plasma levels of the acute phase protein SAA3 were used as a biomarker of systemic acute phase response (Poulsen et al., 2017; Saber et al., 2014). Exposure to FINE NFC at both doses resulted in increased plasma levels of SAA3 on day 1. AS (−COOH) only resulted in increased SAA3 levels at the highest dose. The responses induced by FINE NFC were higher than those observed for AS (−COOH). On day 28, only FINE NFC at the lowest dose increased SAA3 (Fig. 2).

3.4. DNA damage

DNA damage was assessed by the comet assay using both as tail length and as the percentage of DNA in the comet tail of single cells (% DNA). On day 1, exposure to FINE NFC at both tested doses (6 and 18 µg/mouse) resulted in increased DNA damage in lung, but only when evaluated as %DNA. On day 28, only AS (−COOH) at the highest dose increased DNA damage in BAL, and only when measured as tail length (Table 3). BIOCID FINE NFC exhibited higher DNA damage levels than FINE NFC as measured by % DNA; but the level was not different from control (Table 3).

3.5. Histopathology and labelling of nanofibrillated celluloses

Visualisation of nanofibrillated cellulose 28 days post-exposure by EXG:CBM staining showed that both FINE NFC and AS (−COOH) were located in the alveolar region close to terminal bronchioles (Fig. 3). The cellulose appeared as small aggregates that were often located in macrophages (Fig. 3B, C, E and F), or as aggregates that were larger than macrophages. The latter were more prominent for FINE NFC (Fig. 3B and E) than AS (−COOH). In the liver, there was no evident staining for cellulose using EXG:CBM, suggesting that the nanofibrillated cellulose did not reach the liver after the pulmonary exposure or that the levels in liver were too low to be detected.

There were only minor histopathologic changes in the lungs in the form of marginally increased macrophage activity 28 days after exposure to FINE NFC or to AS (−COOH). No histopathological changes were observed in the liver (BIOCID FINE NFC was not investigated by histopathology).

Table 2
Cellularity of BAL. Data are mean ± SD. The statistical test used was one-way ANOVA with Sidak's multiple comparisons test. ****,***, ** and * designates p values of < 0.0001, < 0.001, < 0.01 and < 0.05, respectively vs. vehicle. ^^^^,^^^, ^^ and ^ designates p values of < 0.0001, < 0.001, < 0.01 and < 0.05 respectively *vs*. corresponding dose of FINE NFC.

	Vehicle 0 μg	FINE NFC 6 μg	18 μg	AS (-COOH) 6 μg	18 μg
Day 1					
Macrophages	54828 ± 24976	35982 ± 16595	35335 ± 8114	54698 ± 22910	54638 ± 13964
Lymphocytes	255 ± 556	453 ± 660	1396 ± 1744**	173 ± 257	340 ± 670
Neutrophils	4381 ± 4580	119065 ± 46207****	162066 ± 65931****	13806 ± 11683^^^^	78727 ± 47601**** ^^^^
Eosinophils	755 ± 1734	5336 ± 3969**	4232 ± 1778	1256 ± 1050	7756 ± 9670****
Epithelial	4137 ± 2648	11 ± 17*	27 ± 29*	7952 ± 6120* ^^^^	7997 ± 7064* ^^^^
Total BAL cells	64868 ± 28361	189286 ± 81794****	230857 ± 84254****	77886 ± 37424^^^	149457 ± 60350*** ^^
Day 28					
Macrophages	43121 ± 16156	71128 ± 20642***	66581 ± 3997**	56255 ± 12552	75333 ± 20844****
Lymphocytes	674 ± 1061	400 ± 449	821 ± 786	2586 ± 5437	231 ± 301
Neutrophils	584 ± 679	3027 ± 2113**	2471 ± 2015*	2368 ± 2733*	1065 ± 839
Eosinophils	2443 ± 6601	346 ± 399	338 ± 895	2164 ± 3999	65 ± 173
Epithelial	5037 ± 3190	5056 ± 1685	3832 ± 1478	4084 ± 1804	4177 ± 2189
Total BAL cells	52100 ± 20771	79957 ± 23220 *	74043 ± 5772	67457 ± 21217	80871 ± 22610**

	Vehicle 0 μg	FINE NFC 18 μg	BIOCID FINE NFC 18 μg
Day 1			
Macrophages	39287 ± 14271	25943 ± 8871	33194 ± 8090
Lymphocytes	243 ± 336	1381 ± 1599	1662 ± 1271
Neutrophils	6277 ± 4654	63581 ± 28401*	112297 ± 41317**** ^
Eosinophils	981 ± 1307	24409 ± 15390*	39340 ± 14924***
Epithelial	3610 ± 3890	4169 ± 4219	6174 ± 4999
Total BAL cells	50400 ± 19665	119483 ± 50170***	192667 ± 59258*

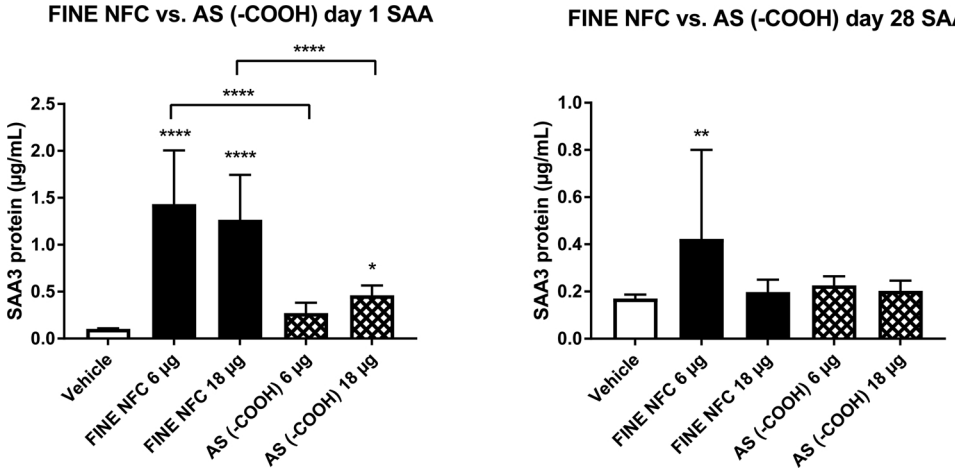

Fig. 2. SAA3 levels in plasma at 1 and 28 days of exposure to FINE NFC or AS (−COOH). FINE NFC and AS (−COOH) were administered by intratracheal instillation to mice at 6 or 18 µg/mouse. 1 or 28 days after exposure, the mice were humanely killed, and the SAA3 protein level was measured in blood plasma by the use of ELISA assay. The values represent mean of all animals in the group ± SD (n = 7).). ****,***, ** and * designates p values of < 0.0001, < 0.001, < 0.01 and < 0.05 respectively *vs.* vehicle or in case of the insertion of a lateral bar: treatment vs. treatment by Sidak's multiple comparisons test (one-way ANOVA).

4. Discussion

4.1. Systemic acute phase response

We found that pulmonary exposure to nanofibrillated cellulose induced increased systemic acute phase response in terms of increased plasma levels of SAA3. Even the relatively low dose 6 µg/mouse (0.3 mg/kg) of FINE NFC induced increased SAA3 plasma levels. When comparing to previous data, NFC FINE appears to be more potent than carbon nanotubes in inducing systemic acute phase response (Poulsen et al., 2017, 2015b). Following pulmonary exposure to carbon nanotubes, only the highest dose, 162 µg/mouse, of two different carbon nanotubes increased SAA3 levels in plasma 24 h post-exposure (Poulsen et al., 2015b), whereas in the current study this was observed already at 6 µg of FINE NFC.

SAA is causally related to atherosclerosis and increased SAA3 plasma levels have been shown to induce increased formation of plaques in aorta of APOE$^{-/-}$ mice (Thompson 2018), a commonly used model of atherosclerosis. Paper production is one of the anticipated uses of nanofibrillated cellulose. In a study of occupational exposure to dust at a Swedish pulp and paper mill, associations were consistently found between occupational exposure to paper mill dust and blood levels of SAA and CRP (Westberg et al., 2016). Thus, there is evidence that occupational exposure to cellulose leads to increased systemic acute phase response. Substitutions with less inflammogenic cellulose species may therefore constitute a safe-by-design approach for the development of cellulose products that are safer for the workers.

4.2. Evidence that carboxylation decrease inflammation and acute phase response induced by nanofibrillated cellulose

We aimed at assessing whether blocking of OH groups by carboxylation reduced the toxicity of nanofibrillated celluloses. This seems to be the case, since AS(−COOH) with carboxylated OH groups induced less inflammation in terms of BAL neutrophils and less systemic acute phase response in terms of the plasma level of SAA3 as compared with FINE NFC. BIOCID NFC increased BAL neutrophils to a higher extent than FINE NFC, suggesting that the addition of BIM MC4901 was not involved in the reduced inflammation and acute phase response induced by AS (−COOH). In a previous study also comparing FINE NFC and AS (−COOH) and including two additional nanofibrillated celluloses, one carboxymethylated and the other non-functionalised, a similar effect of functionalisation on pulmonary inflammation was observed (Ilves et al., 2018).

The two nanofibrillated celluloses are not completely similar in size as FINE NFC has dimensions of 2–20 µm in length and 2–15 nm in width whereas AS (−COOH) is 0.5–10 µm in length and 4–10 nm in width. Both nanofibrillated celluloses were readily visualised in lung tissue 28 days post-exposure at comparable levels (Fig. 3) and both often appeared phagocytosed by macrophages. However, aggregates larger than macrophages seemed more prominent for FINE NFC than AS (−COOH), potentially contributing to the more pronounced toxicity of FINE NFC as compared to AS (−COOH). It is possible that these differences in aggregation are influenced by the carboxylation of the nanofibrillated celluloses. We have previously shown that physico-chemical properties of multiwalled carbon nanotubes are determinants of long-term presence of agglomerates in lung tissue after pulmonary dosing in mice (Knudsen et al., 2018).

In the current investigation, we found pulmonary inflammation at both doses (0.3 and 0.9 mg/kg bw) of FINE NFC, but only at the highest dose of AS (−COOH). This suggests that the 0.3 mg/kg bw/day dose is a lowest-observed-adverse-effect level (LOAEL) for FINE NFC and a no-observed-adverse-effect level (NOAEL) for AS (−COOH). Similarly, our data on systemic SAA3 suggested a LOAEL of 0.3 mg/kg bw for FINE NFC, and our results on AS (−COOH) indicates that 0.3 mg/kg bw is the NOAEL. Ilves et al. previously investigated the pulmonary inflammation of five celluloses, including two materials also investigated in the current study, FINE NFC and AS (−COOH). All 5 materials increased the number of neutrophils in BAL (at both doses ˜0.5 and ˜2 mg/kg bw), suggesting a LOAEL of 0.5 mg/kg bw (Ilves et al., 2018). Mice exposed to 2,2,6,6-tetramethyl-piperidin-1-oxyl oxidised nanofibrillated cellulose had increased BAL neutrophils at high doses of 80 and 200 µg, but not at lower doses of 10 and 40 µg/mouse, indicating a NOAEL of 2 mg/kg bw (Catalán et al., 2017). Pulmonary exposure of mice to cellulose nanocrystals (10 µg/mouse, 2 times per week for 3 weeks) by pharyngeal aspiration resulted in pulmonary inflammation, suggesting a LOAEL of 3 mg/kg bw (Shvedova et al., 2016). Exposure of mice to cellulose nanocrystals derived from wood increased the number of leukocytes and eosinophils in BAL. The doses were 50, 100, and 200 µg/mouse administered by pharyngeal aspiration, suggesting a LOAEL of 2.5 mg/kg bw (Yanamala et al., 2014). Taken together, we observed pulmonary inflammation for non-carboxylated nanofibrillated cellulose at lower doses than what has previously been observed (LOAEL of 0.3 mg/kg bw). In addition, we found a NOAEL for carboxylated AS (−COOH) at 0.3 mg/kg bw, whereas Ilves et al. (2018) obtained a LOAEL of 0.5 mg/kg bw for the same material. These differences in inflammatory responses may be explained by the exposure methods used. Ilves et al. (2018) exposed mice by aspiration, while we used intratracheal instillation. Since nanofibrillated cellulose in dispersion is viscous, dosing by intratracheal instillation may result in a more efficient alveolar dosing than aspiration, and this may be the reason for the differences in inflammatory responses between the present and the previous study. However, both we and Ilves et al. (2018) found the non-carboxylated nanofibrillated cellulose to have a higher

Table 3
DNA damage in BAL fluid cells, lung and liver tissue 1 and 28 days after exposure to FINE NFC, AS (−COOH) or BIOCID FINE NFC. TL, comet tail length; %TDNA, percentage DNA in the comet tail. Data are mean ± SD. The statistical test used was one-way ANOVA with Sidak's multiple comparisons test. ** and * designates p values of < 0.01 and < 0.05 respectively vs. vehicle. ^ designates a p value of < 0.05 vs. corresponding dose of FINE NFC.

	Vehicle 0 μg	Fine NFC 6 μg	18 μg	AS (-COOH) 6 μg	18 μg
Day 1					
BAL TL	10.7 ± 3.9	12.0 ± 1.3	11.3 ± 1.0	13.2 ± 1.6	11.1 ± 0.8
BAL %TDNA	4.2 ± 2.7	4.3 ± 0.8	3.8 ± 0.7	5.4 ± 1.1	4.0 ± 0.5
Lung TL	12.2 ± 2.4	14.6 ± 1.8	13.9 ± 1.9	13.5 ± 2.8	12.5 ± 2.0
Lung %TDNA	3.7 ± 1.3	5.2 ± 1.2*	5.1 ± 1.1*	5.0 ± 1.4	4.2 ± 1.1
Liver TL	11.4 ± 2.7	10.5 ± 0.9	10.1 ± 1.2	10.4 ± 1.1	10.6 ± 1.5
Liver %TDNA	2.9 ± 1.8	3.1 ± 0.4	2.7 ± 0.6	2.9 ± 0.7	3.0 ± 0.8
Day 28					
BAL TL	10.7 ± 3.9	12.0 ± 1.3	11.3 ± 1.0	13.2 ± 1.6	11.1 ± 0.8*
BAL %TDNA	4.2 ± 2.7	4.3 ± 0.8	3.8 ± 0.7	5.4 ± 1.1	4.0 ± 0.5
Lung TL	15.3 ± 4.5	14.6 ± 1.8	13.9 ± 1.9	13.5 ± 2.8	12.5 ± 2.0
Lung %TDNA	6.5 ± 4.0	5.2 ± 1.2	5.1 ± 1.1	5.0 ± 1.4	4.2 ± 1.1
Liver TL	15.1 ± 5.4	10.5 ± 0.9	10.1 ± 1.2	10.4 ± 1.1	10.6 ± 1.5
Liver %TDNA	7.8 ± 8.0	3.1 ± 0.4	2.7 ± 0.6	2.9 ± 0.7	3.0 ± 0.8

	Vehicle 0 μg	FINE NFC 18 μg	BIOCID FINE NFC 18 μg
Day 1			
BAL TL	8.7 ± 0.7	7.3 ± 0.6**	7.3 ± 0.3**
BAL %TDNA	3.2 ± 0.5	2.7 ± 0.6	3.2 ± 0.5
Lung TL	14.1 ± 4.1	13.1 ± 2.5	11.6 ± 0.8
Lung %TDNA	6.9 ± 7.6	4.9 ± 1.9	4.0 ± 0.9
Liver TL	9.1 ± 1.0	9.5 ± 1.6	9.4 ± 1.4
Liver %TDNA	1.8 ± 0.4	1.7 ± 0.3	2.2 ± 0.3^

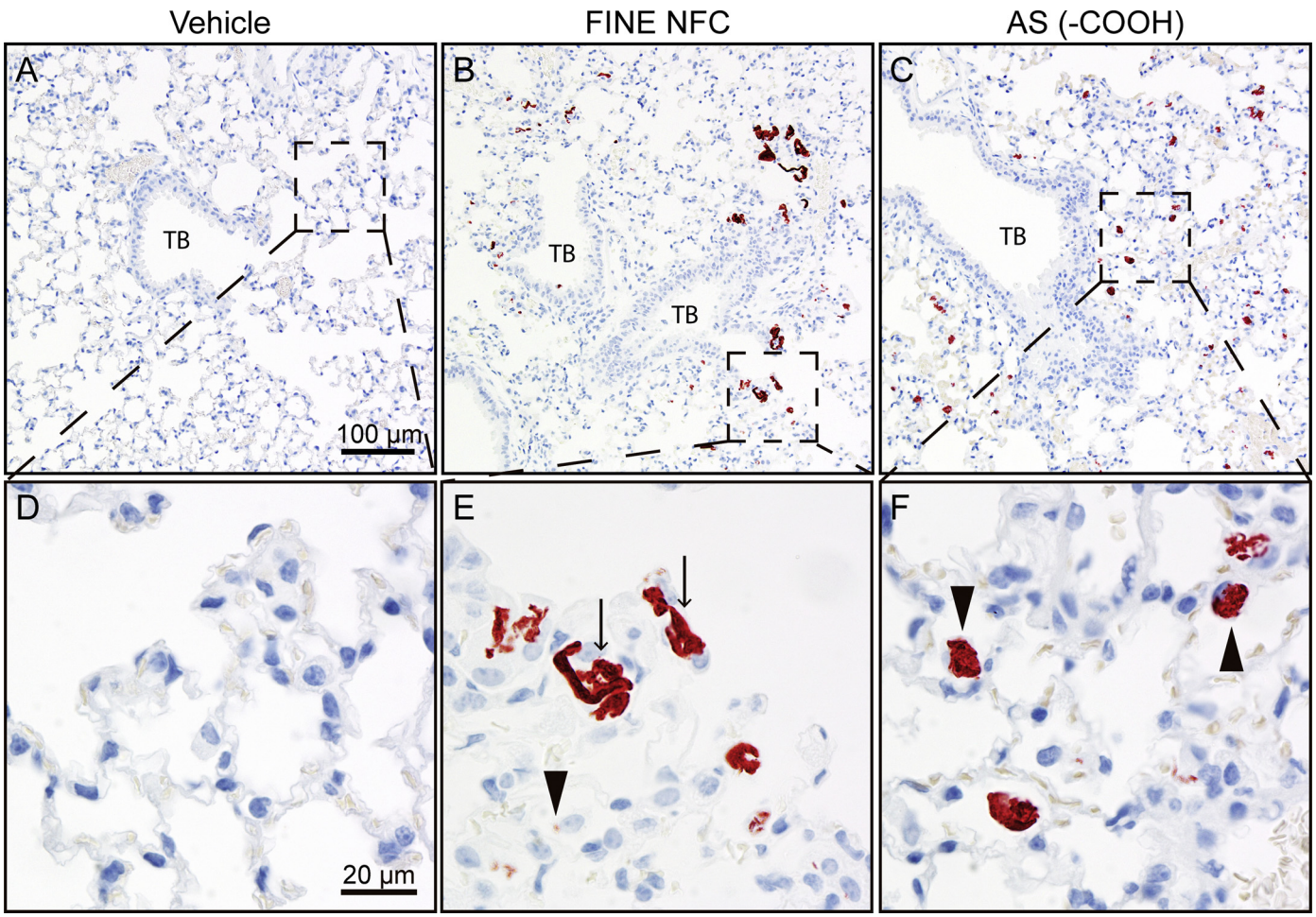

Fig. 3. Distribution of FINE NFC and AS (−COOH) in lung tissue. FINE NFC and AS (−COOH) were administered by intratracheal instillation to mice at 18 µg/mouse. 28 days after exposure, nanofibrillated cellulose in the lungs were labelled with EXG:CBM (red) and tissue were counterstained with haematoxylin (blue). TB designates: terminal bronchiole; arrows indicate the location of large aggregates of nanofibrillated cellulose; arrow heads indicate the location of aggregates of nanofibrillated cellulose in macrophages. Scale bar 100 µm in A–C and 20 µm in.D–F.

toxicity compared to the carboxylated AS (−COOH) in head-to-head comparisons, suggesting that carboxylation indeed lowers the toxicity.

4.3. Effects of nanofibrillated cellulose on DNA damage

We observed increased DNA damage induced by FINE NFC and AS (−COOH). For AS (−COOH) this was observed in BAL and for FINE NFC in lung tissue. This indicates that these two materials have a genotoxic potential, although no dose-response relationship was observed. There were no effects of the nanofibrillated celluloses on the liver. This is consistent with the absence of cellulose-specific staining by EXG:CBM of FINE NFC in the liver, indicating that nanofibrillated celluloses do not reach this tissue. We have previously suggested that the mechanism underlying carbon black nanoparticles-induced DNA damage in the liver is by primary genotoxicity and this suggests that translocation is required for liver genotoxicity (Modrzynska et al., 2018), and the present findings would be consistent with this.

Previously, DNA damage was observed in lung tissue after the exposure of mice to 2,2,6,6-tetramethyl-piperidin-1-oxyl oxidised nanofibrillated cellulose. This was observed at aspiration doses 10 and 40 µ/mouse, but not at higher tested doses 80 and 200 µg/mouse (Catalán et al., 2017). In addition, oxidative stress induction was observed in mice exposed to cellulose nanocrystals by pharyngeal aspiration at 10 µg/mouse (2 times a week for 3 weeks) (Shvedova et al., 2016). Taken together, our results and the results of other groups indicate a genotoxic potential for nano-fibrillated cellulose. This is in line with data on the mother-compound, cellulose. Exposure to wood dust (in which cellulose is the major constituent) causes cancer of the nose and the paranasal sinuses (IARC, 1995), and exposure to textile fibres in weavers has also been considered possibly carcinogenic (Muhle and Ernst, 1997; IARC, 1990). Overall, genotoxicity and cancer are endpoints that have to be considered when evaluating the toxicity of cellulose and nanofibrillated cellulose.

5. Conclusions

Pulmonary exposure to nanofibrillated cellulose induced pulmonary inflammation and genotoxicity and systemic acute phase response. The carboxylated nanofibrillated cellulose induced lower neutrophil numbers in BAL and lower systemic acute phase response than the unmodified nanofibrillated cellulose, suggesting that carboxylation of the OH groups reduces the nanofibrillated cellulose-induced systemic acute phase response. Functionalisation of the OH groups may therefore be a strategy to lower the pulmonary toxicity of these materials. Genotoxicity was observed across materials, doses and time points. The lowest tested dose used, 0.3 mg/kg bw, could be suggested as a LOAEL for FINE NFC and as a NOAEL for AS (−COOH).

Transparency document

The Transparency document associated with this article can be found in the online version.

Acknowledgements

This work was supported by the European Union Seventh Framework Program (FP7/2007-2013) under the project NANoREG (A common European approach to the regulatory testing of nanomaterials), grant agreement 310584, Danish Centre for Nanosafety 2, and the Danish Centre for Nanosafety, grant# 20110092173-3 from the Danish Working Environment Research Foundation. Technical assistance from Michael Guldbrandsen, Eva Terrida, Natacha Synnøve Olsen, Inge Christiansen, Ulla Tegner, Anne-Karin Asp, and Zdenka Kyjovska was greatly appreciated.

References

Bengtson, S., Knudsen, K.B., Kyjovska, Z.O., Berthing, T., Skaug, V., Levin, M., Koponen, I.K., Shivayogimath, A., Booth, T.J., Alonso, B., Pesquera, A., Zurutuza, A., Thomsen, B.L., Troelsen, J.T., Jacobsen, N.R., Vogel, U., 2017. Differences in inflammation and acute phase response but similar genotoxicity in mice following pulmonary exposure to graphene oxide and reduced graphene oxide. PLoS One 12, e0178355.

Bourdon, J.A., Saber, A.T., Jacobsen, N.R., Jensen, K.A., Madsen, A.M., Lamson, J.S., Wallin, H., Moller, P., Loft, S., Yauk, C.L., Vogel, U.B., 2012. Carbon black nanoparticle instillation induces sustained inflammation and genotoxicity in mouse lung and liver. Part Fibre Toxicol. 9, 5.

Catalán, J., Rydman, E., Aimonen, K., Hannukainen, K.-S., Suhonen, S., Vanhala, E., Moreno, C., Meyer, V., Perez, D., da, S., Sneck, A., Forsström, U., Højgaard, C., Willemoes, M., Winther, J.R., Vogel, U., Wolff, H., Alenius, H., Savolainen, K.M., Norppa, H., 2017. Genotoxic and inflammatory effects of nanofibrillated cellulose in murine lungs. Mutagenesis 32, 23–31. https://doi.org/10.1093/mutage/gew035.

Cullen, R.T., Searl, A., Miller, B.G., Davis, J.M., Jones, A.D., 2000. Pulmonary and intraperitoneal inflammation induced by cellulose fibres. J. Appl. Toxicol. 20, 49–60.

Dong, Z., Wu, T., Qin, W., An, C., Wang, Z., Zhang, M., Zhang, Y., Zhang, C., An, F., 2011. Serum amyloid A directly accelerates the progression of atherosclerosis in apolipoprotein E-deficient mice. Mol. Med. 17, 1357–1364. https://doi.org/10.2119/molmed.2011.00186.

ECHA, E., 2013. Database on ECHA Registered Substances [WWW Document].

Farcas, M.T., Kisin, E.R., Menas, A.L., Gutkin, D.W., Star, A., Reiner, R.S., Yanamala, N., Savolainen, K., Shvedova, A.A., 2016. Pulmonary exposure to cellulose nanocrystals caused deleterious effects to reproductive system in male mice. J. Toxicol. Environ. Health A 79, 984–997. https://doi.org/10.1080/15287394.2016.1211045.

Gabay, C., Kushner, I., 1999. Acute-phase proteins and other systemic responses to inflammation. N. Engl. J. Med. 340, 448–454. https://doi.org/10.1056/NEJM199902113400607.

Gómez, H.C., Serpa, A., Velásquez-Cock, J., Gañán, P., Castro, C., Vélez, L., Zuluaga, R., 2016. Vegetable nanocellulose in food science: a review. Food Hydrocoll. 57, 178–186. https://doi.org/10.1016/j.foodhyd.2016.01.023.

Halappanavar, S., Jackson, P., Williams, A., Jensen, K.A., Hougaard, K.S., Vogel, U., Yauk, C.L., Wallin, H., 2011. Pulmonary response to surface-coated nanotitanium dioxide particles includes induction of acute phase response genes, inflammatory cascades, and changes in microRNAs: a toxicogenomic study. Environ. Mol. Mutagen. 52, 425–439.

IARC, 1990. Some flame retardants and textile chemicals, and exposures in the textile manufacturing industry. IARC Monogr. Eval. Carcinog. Risks Hum. 48, 1–278.

IARC, 1995. IARC Monographs on the Evaluation of Carcinogenic Risks to Humans. Wood Dust and Formaldehyde. IARC Monogr. Eval. Carcinog. Risks to Humans 62.

Ilves, M., Vilske, S., Aimonen, K., Lindberg, H.K., Pesonen, S., Wedin, I., Nuopponen, M., Vanhala, E., Højgaard, C., Winther, J.R., Willemoës, M., Vogel, U., Wolff, H., Norppa, H., Savolainen, K., Alenius, H., 2018. Nanofibrillated cellulose causes acute pulmonary inflammation that subsides within a month. Nanotoxicology 12, 729–746. https://doi.org/10.1080/17435390.2018.1472312.

Jackson, P., Pedersen, L.M., Kyjovska, Z.O., Jacobsen, N.R., Saber, A.T., Hougaard, K.S., Vogel, U., Wallin, H., 2013. Validation of freezing tissues and cells for analysis of DNA strand break levels by comet assay. Mutagenesis 28, 699–707. https://doi.org/10.1093/mutage/get049.

Jacobsen, N.R., Moller, P., Jensen, K.A., Vogel, U., Ladefoged, O., Loft, S., Wallin, H., 2009. Lung inflammation and genotoxicity following pulmonary exposure to nanoparticles in ApoE-/- mice. Part Fibre Toxicol. 6, 2.

Johnson, R.K., Zink-Sharp, A., Renneckar, S.H., Glasser, W.G., 2009. A new bio-based nanocomposite: fibrillated TEMPO-oxidized celluloses in hydroxypropylcellulose matrix. Cellulose 16, 227–238. https://doi.org/10.1007/s10570-008-9269-6.

Knudsen, K.B., Kofoed, C., Espersen, R., Hojgaard, C., Winther, J.R., Willemoes, M., Wedin, I., Nuopponen, M., Vilske, S., Aimonen, K., Weydahl, I.E., Alenius, H., Norppa, H., Wolff, H., Wallin, H., Vogel, U., 2015. Visualization of nanofibrillar cellulose in biological tissues using a biotinylated carbohydrate binding module of beta-1,4-glycanase. Chem. Res. Toxicol. 28, 1627–1635.

Knudsen, K.B., Berthing, T., Jackson, P., Poulsen, S.S., Mortensen, A., Jacobsen, N.R., Skaug, V., Szarek, J., Hougaard, K.S., Wolff, H., Wallin, H., Vogel, U., 2018. Physicochemical predictors of Multi-Walled Carbon Nanotube-induced pulmonary histopathology and toxicity one year after pulmonary deposition of 11 different Multi-Walled Carbon Nanotubes in mice. Basic Clin. Pharmacol. Toxicol. 1–17. https://doi.org/10.1111/bcpt.13119.

Milton, D.K., Godleski, J.J., Feldman, H.A., Greaves, I.A., 1990. Toxicity of intratracheally instilled cotton dust, cellulose, and endotoxin. Am. Rev. Respir. Dis. 142, 184–192. https://doi.org/10.1164/ajrccm/142.1.184.

Modrzynska, J., Berthing, T., Ravn-Haren, G., Jacobsen, N.R., Weydahl, I.K., Loeschner, K., Mortensen, A., Saber, A.T., Vogel, U., 2018. Primary genotoxicity in the liver following pulmonary exposure to carbon black nanoparticles in mice. Part. Fibre Toxicol. 15, 2. https://doi.org/10.1186/s12989-017-0238-9.

Muhle, H., Ernst, H., Bellmann, B., 1997. Investigation of the durability of cellulose fibres in rat lungs. Ann. Occup. Hyg. 41, 184–188.

Poulsen, S.S., Saber, A.T., Mortensen, A., Szarek, J., Wu, D., Williams, A., Andersen, O., Jacobsen, N.R., Yauk, C.L., Wallin, H., Halappanavar, S., Vogel, U., 2015a. Changes in cholesterol homeostasis and acute phase response link pulmonary exposure to multi-walled carbon nanotubes to risk of cardiovascular disease. Toxicol. Appl. Pharmacol. 283, 210–222.

Poulsen, S.S., Saber, A.T., Williams, A., Andersen, O., Kobler, C., Atluri, R., Pozzebon, M.E., Mucelli, S.P., Simion, M., Rickerby, D., Mortensen, A., Jackson, P., Kyjovska, Z.O., Molhave, K., Jacobsen, N.R., Jensen, K.A., Yauk, C.L., Wallin, H., Halappanavar, S., Vogel, U., 2015b. MWCNTs of different physicochemical properties cause similar inflammatory responses, but differences in transcriptional and histological markers of fibrosis in mouse lungs. Toxicol. Appl. Pharmacol. 284, 16–32.

Poulsen, S.S., Knudsen, K.B., Jackson, P., Weydahl, I.E.K., Saber, A.T., Wallin, H., Vogel, U., 2017. Multi-walled carbon nanotube-physicochemical properties predict the systemic acute phase response following pulmonary exposure in mice. PLoS One 12, e0174167. https://doi.org/10.1371/journal.pone.0174167.

Ridker, P.M., Hennekens, C.H., Buring, J.E., Rifai, N., 2000. C-reactive protein and other markers of inflammation in the prediction of cardiovascular disease in women. N. Engl. J. Med. 342, 836–843. https://doi.org/10.1056/NEJM200003233421202.

Rylander, R., Schilling, R.S., Pickering, C.A., Rooke, G.B., Dempsey, A.N., Jacobs, R.R., 1987. Effects after acute and chronic exposure to cotton dust: the Manchester criteria. Br. J. Ind. Med. 44, 577–579.

Saber, A.T., Lamson, J.S., Jacobsen, N.R., Ravn-Haren, G., Hougaard, K.S., Nyendi, A.N., Wahlberg, P., Madsen, A.M., Jackson, P., Wallin, H., Vogel, U., 2013. Particle-induced pulmonary acute phase response correlates with neutrophil influx linking inhaled particles and cardiovascular risk. PLoS One 8, e69020.

Saber, A.T., Jacobsen, N.R., Jackson, P., Poulsen, S.S., Kyjovska, Z.O., Halappanavar, S., Yauk, C.L., Wallin, H., Vogel, U., 2014. Particle-induced Pulmonary Acute Phase Response may be the Causal Link Between Particle Inhalation and Cardiovascular Disease. Wiley Interdiscip. Rev. Nanomed. Nanobiotechnol. 6, 517–531.

Shvedova, A.A., Kisin, E.R.E.R., Yanamala, N., Farcas, M.T., Menas, A.L., Williams, A., Fournier, P.M., Reynolds, J.S., Gutkin, D.W., Star, A., Reiner, R.S., Halappanavar, S., Kagan, V.E., 2016. Gender differences in murine pulmonary responses elicited by cellulose nanocrystals. Part. Fibre Toxicol. 13, 28. https://doi.org/10.1186/s12989-016-0140-x.

Thompson, J.C., Wilson, P.G., Shridas, P., Ji, A., de Beer, M., de Beer, F.C., Webb, N.R., Tannock, L.R., 2018. Serum amyloid A3 is pro-atherogenic. Atherosclerosis 268, 32–35. https://doi.org/10.1016/j.atherosclerosis.2017.11.011.

Vartiainen, J., Pöhler, T., Sirola, K., Pylkkänen, L., Alenius, H., Hokkinen, J., Tapper, U., Lahtinen, P., Kapanen, A., Putkisto, K., Hiekkataipale, P., Eronen, P., Ruokolainen, J., Laukkanen, A., 2011. Health and environmental safety aspects of friction grinding and spray drying of microfibrillated cellulose. Cellulose 18, 775–786. https://doi.org/10.1007/s10570-011-9501-7.

Westberg, H., Elihn, K., Andersson, E., Persson, B., Andersson, L., Bryngelsson, I.-L., Karlsson, C., Sjögren, B., 2016. Inflammatory markers and exposure to airborne particles among workers in a Swedish pulp and paper mill. Int. Arch. Occup. Environ. Health 89, 813–822. https://doi.org/10.1007/s00420-016-1119-5.

Yanamala, N., Farcas, M.T., Hatfield, M.K., Kisin, E.R., Kagan, V.E., Geraci, C.L., Shvedova, A.A., 2014. In vivo evaluation of the pulmonary toxicity of cellulose nanocrystals: a renewable and sustainable nanomaterial of the future. ACS Sustain. Chem. Eng. 2, 1691–1698. https://doi.org/10.1021/sc500153k.